

Supporting Information

Title: Influence of aqueous solutions of 2-(tetrafluoro(trifluoromethyl)-λ⁶-sulfanyl-ethan-1-ol (CF₃SF₄-ethanol) on the stabilization of the secondary structure of melittin: Comparison with aqueous trifluoroethanol using molecular dynamics simulations and circular dichroism experiments.

Samadrita Biswas¹, Nilavra Pathak², Leah Sutherland¹, Alan Chen^{1,3*}, John T. Welch^{1*}

¹Department of Chemistry, University at Albany, State University of New York, 1400 Washington Ave, Albany, NY 12222, USA

²Marketing Data Science, Expedia Group, 350 Fifth Ave, 7220, New York 10118

³RNA Institute, University at Albany, State University of New York, 1400 Washington Ave, Albany, NY 12222, USA

Alan A. Chen – achen6@albany.edu

John T. Welch – jwelch@albany.edu

* Corresponding author

Table of Contents

Figure S1. Secondary structure count for melittin (MLT) with respect of simulation time in CF ₃ SF ₄ -ethanol different concentrations.	S4
Figure S2. Secondary structure count for melittin (RMLT) with respect of simulation time in CF ₃ SF ₄ -ethanol for different concentrations.	S5
Figure S3. Secondary structure count for melittin (MLT) with respect of simulation time in TFE different concentrations.	S6
Figure S4. Secondary structure count for melittin (RMLT) with respect of simulation time in TFE.	S7
Figure S5. Representative snapshot of simulation within 0.6 nm from the melittin (MLT) backbone in CF ₃ SF ₄ -ethanol-water system. PDB: 2MLT of melittin at 0.5 % (a), 1 % (c), 2.5 % (e), 4.5 % (g), and 6 % (i) of CF ₃ SF ₄ -ethanol-water system at the beginning of simulation. α -helix of melittin after 50 ns simulation in 0.5 % (b), 1 % (d), 2.5 % (f), 4.5 % (h), and 6 % (j) CF ₃ SF ₄ -ethanol-water system.	S8
Figure S6. Representative snapshot of simulation within 0.6 nm from the melittin (MLT) backbone in TFE-water system. PDB: 2MLT of melittin at 8 % (a), 10 % (c), 20 % (e), and 30 % (g) TFE-water system at the beginning of simulation. α -helix of melittin after 50 ns simulation in 8 % (b), 10 % (d), 20 % (f), and 30 % (h) TFE-water system.	S9
Figure S7. Representative snapshot of simulation within a distance of 0.6 nm from the melittin (RMLT) backbone in CF ₃ SF ₄ -ethanol-water system. Random coil structure of melittin at the beginning of simulation at 0.5 % (a) , 2.5 % (c) , 4.5 % (e) , and 6 %.	S10
Figure S8. Representative snapshot of simulation within 0.6 nm from the melittin (RMLT) backbone in TFE-water system. Random coil structure of melittin at 10 % (a), 20 % (c), and 30 % (e) TFE-water system at the beginning of simulation. α -helix of melittin after 50 ns simulation in 10 % (b), 20 % (d) and 30 % (f) TFE-water system.	S11
Figure S9. Backbone RMSD with respect to the initial simulated structure RMLT in 1%, 8% CF ₃ SF ₄ -ethanol-water and 8% and 40% TFE-water system for 50 ns simulation time.	S12
Figure S10. Backbone RMSD with respect to the initial structure of simulation of melittin (MLT) in CF ₃ SF ₄ -ethanol for different concentrations.	S13
Figure S11. Backbone RMSD with respect to the initial structure of simulation of melittin (RMLT) in CF ₃ SF ₄ -ethanol for different concentrations.	S14
Figure S12. Backbone RMSD with respect to the initial structure of simulation of melittin (MLT) in TFE for different concentrations.	S15
Figure S13. Backbone RMSD with respect to the initial structure of simulation of melittin (RMLT) in TFE for different concentrations.	S16
Figure S14. Folding of RMLT in 8% CF ₃ SF ₄ -ethanol from 50 ns simulation.	S17

Figure S15. Backbone RMSF with respect to the structure RMLT in 1%, 8% CF ₃ SF ₄ -ethanol-water and 8% and 40% TFE-water system with respect to residue number.	S18
Figure S16. Backbone RMSF with respect to the initial structure of simulation of melittin (MLT) in, CF ₃ SF ₄ -ethanol for different concentrations.	S19
Figure S17. Backbone RMSF with respect to the initial structure of simulation of melittin (RMLT) in CF ₃ SF ₄ -ethanol for different concentrations.	S20
Figure S18. Backbone RMSF with respect to the initial structure of simulation of melittin (MLT) in TFE for different concentrations.	S21
Figure S19. Backbone RMSF with respect to the initial structure of simulation of melittin (RMLT) in TFE for different concentrations.	S22
Figure S20. Helicity per residue with respect to % of time of melittin (MLT) in CF ₃ SF ₄ -ethanol for different concentrations.	S23
Figure S21. Helicity per residue with respect to % of time of melittin (RMLT) in CF ₃ SF ₄ -ethanol for different concentrations.	S24
Figure S22. Helicity per residue with respect to % of time of melittin (MLT) in TFE for different concentrations.	S25
Figure S23. Helicity per residue with respect to % of time of melittin (RMLT) in TFE for different concentrations.	S26
Figure S24. Intermolecular hydrogen bonding interactions between the alcohols and the peptide over the period of the simulations.	S27

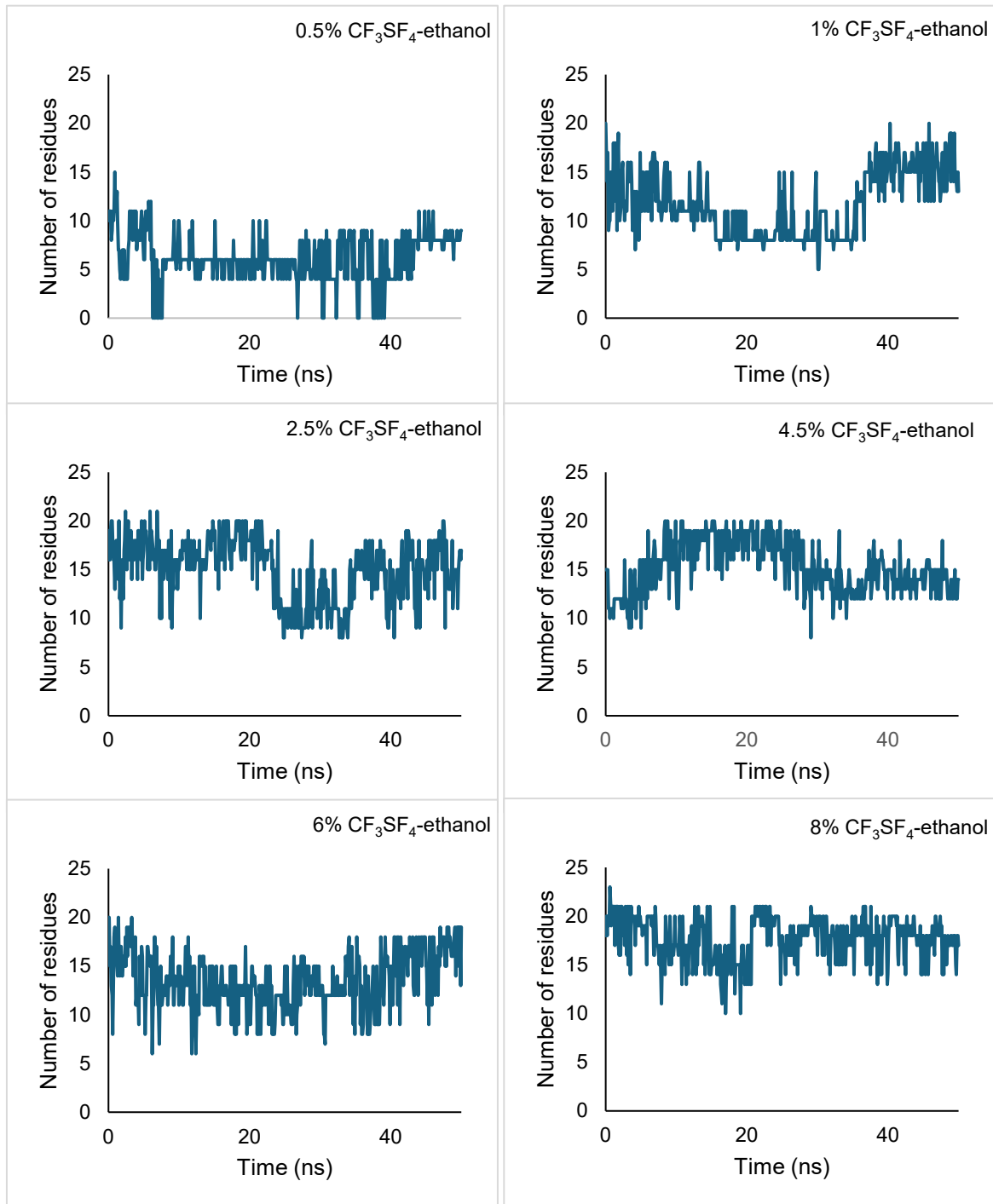


Figure S1. Secondary structure count for melittin (MLT) with respect of simulation time in CF_3SF_4 -ethanol different concentrations.

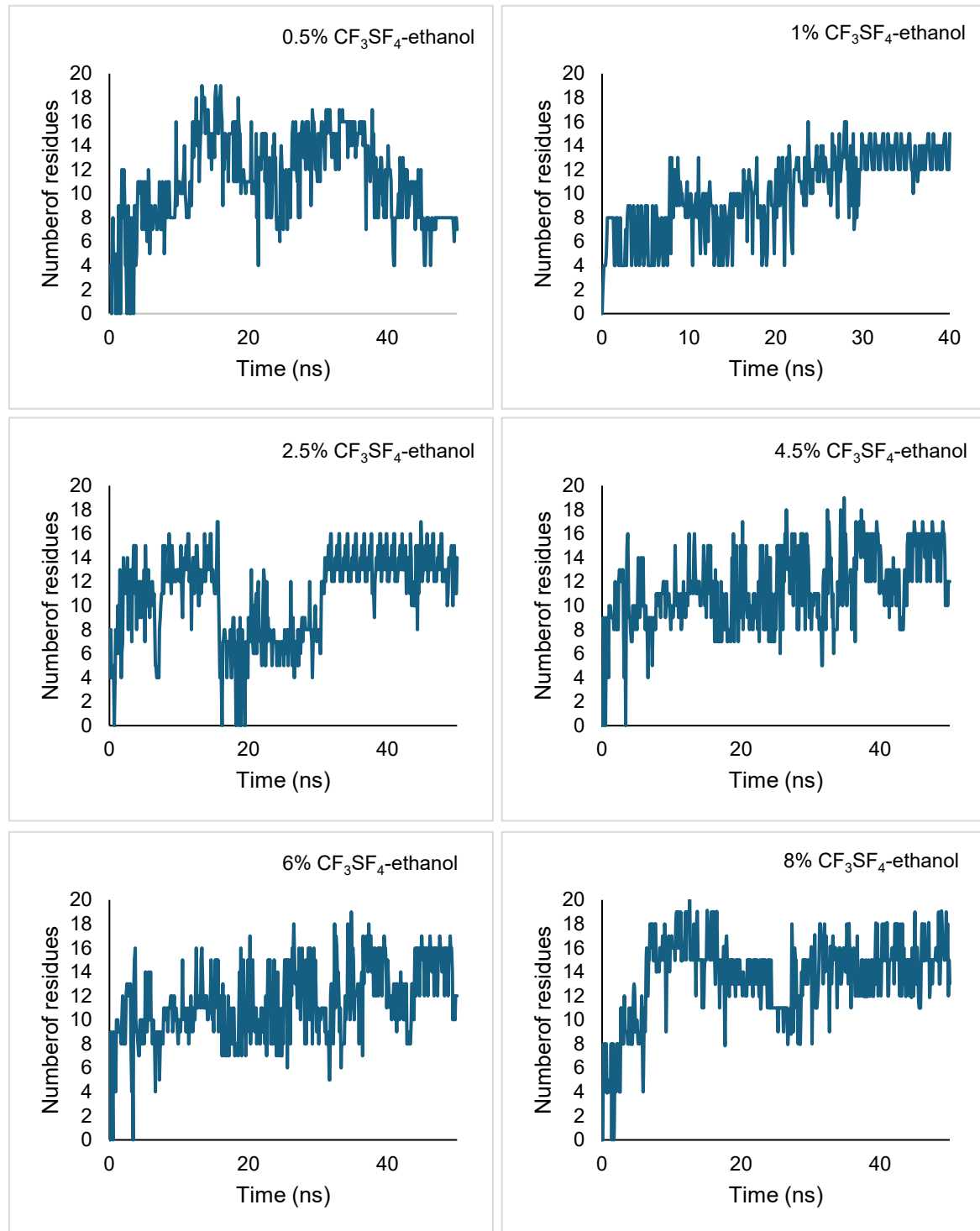


Figure S2. Secondary structure count for melittin (RMLT) with respect of simulation time in CF_3SF_4 -ethanol for different concentrations.

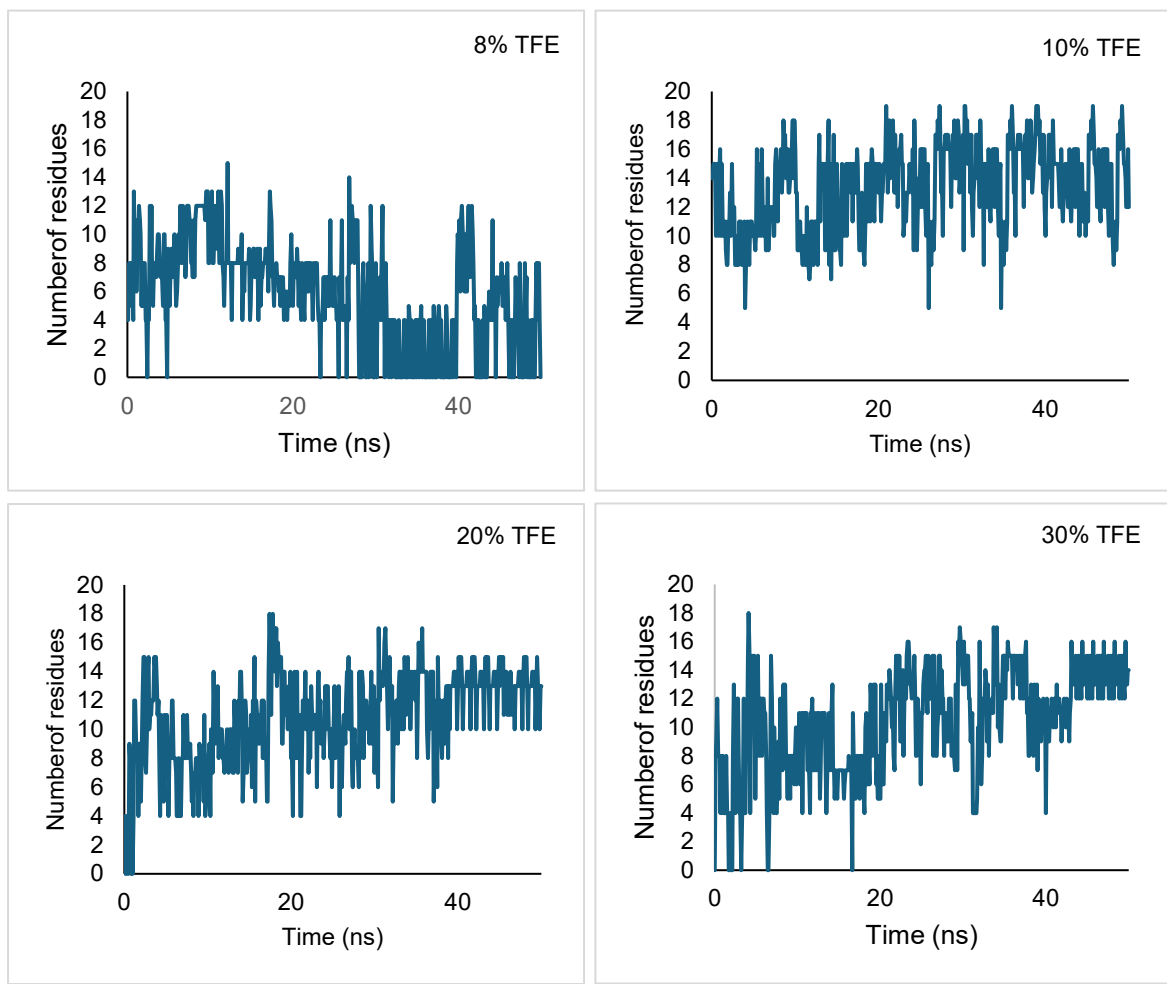


Figure S3. Secondary structure count for melittin (MLT) with respect of simulation time in TFE different concentrations.

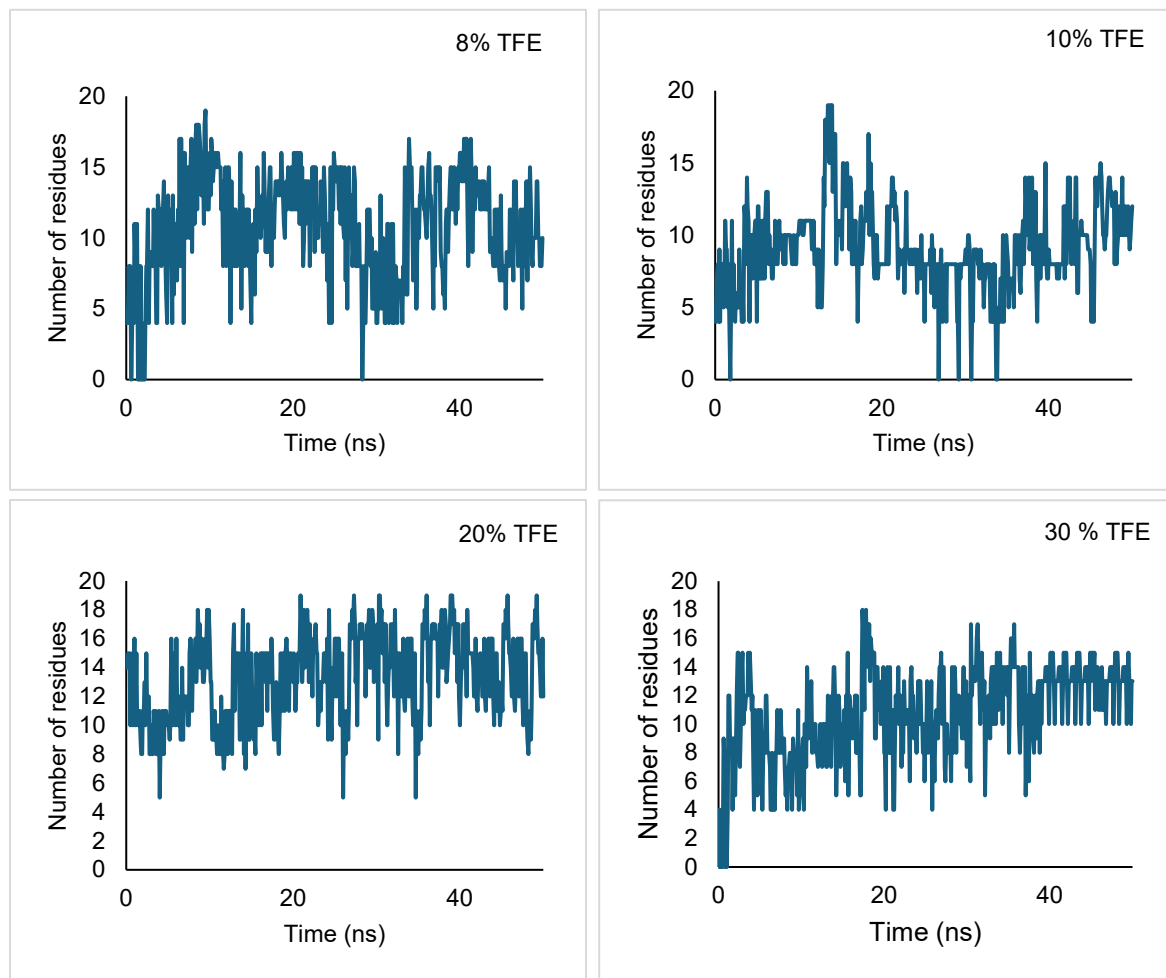


Figure S4. Secondary structure count for melittin (RMLT) with respect of simulation time in TFE.

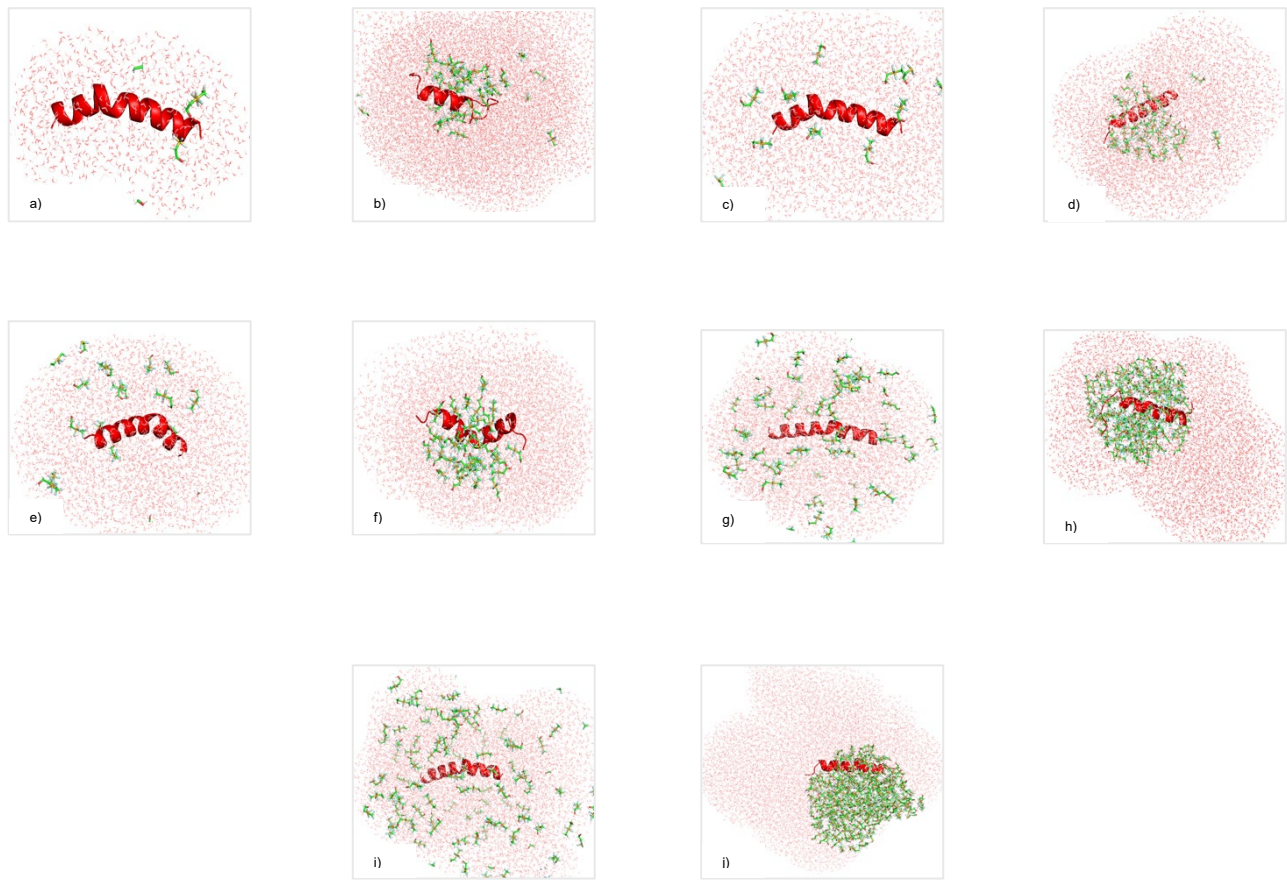


Figure S5. Representative snapshot of simulation within 0.6 nm from the melittin (MLT) backbone in CF_3SF_4 -ethanol-water system. PDB: 2MLT of melittin at 0.5 % (a), 1 % (c), 2.5 % (e), 4.5 % (g), and 6 % (i) of CF_3SF_4 -ethanol-water system at the beginning of simulation. α -helix of melittin after 50 ns simulation in 0.5 % (b), 1 % (d), 2.5 % (f), 4.5 % (h), and 6 % (j) CF_3SF_4 -ethanol-water system.

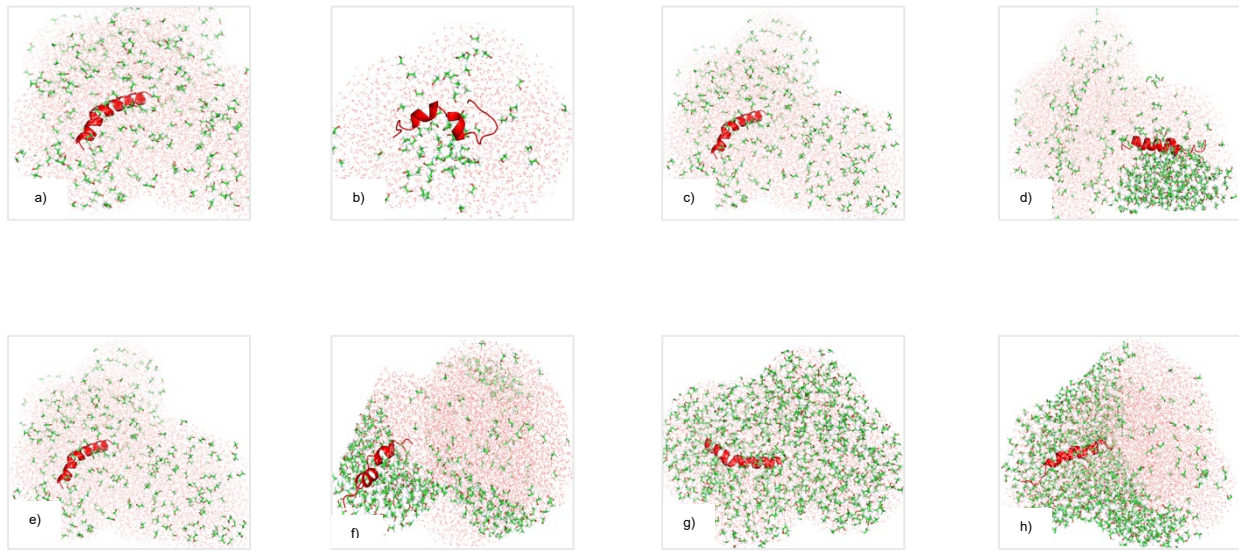


Figure S6. Representative snapshot of simulation within 0.6 nm from the melittin (MLT) backbone in TFE-water system. PDB: 2MLT of melittin at 8 % (a), 10 % (c), 20 % (e), and 30 % (g) TFE-water system at the beginning of simulation. α -helix of melittin after 50 ns simulation in 8 % (b), 10 % (d), 20 % (f), and 30 % (h) TFE-water system.

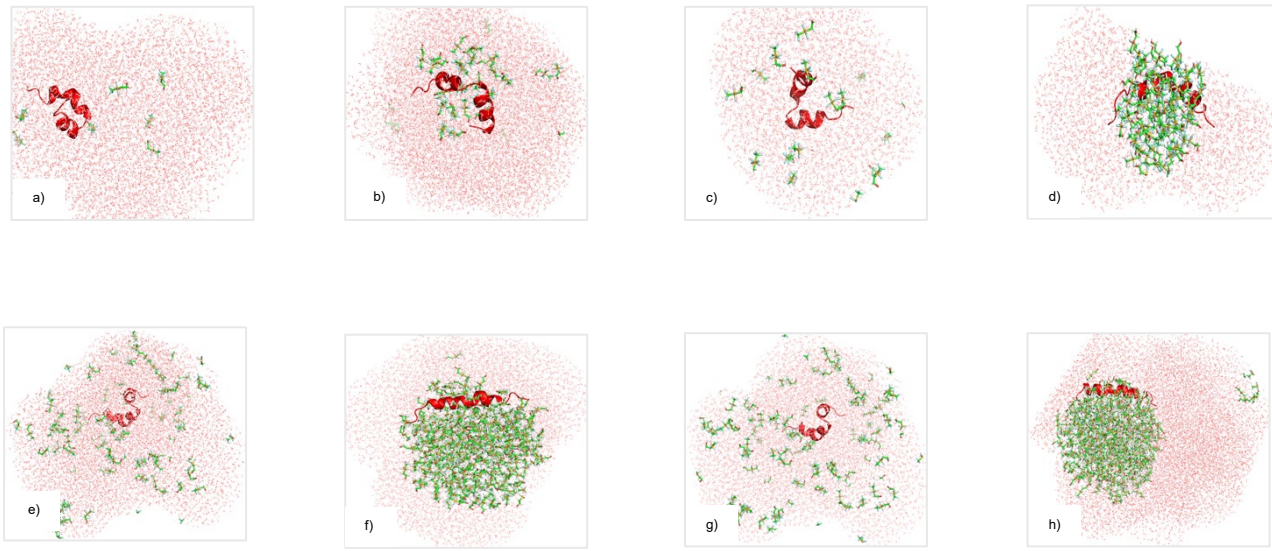


Figure S7. Representative snapshot of simulation within a distance of 0.6 nm from the melittin (RMLT) backbone in CF3SF4 -ethanol-water system. Random coil structure of melittin at the beginning of simulation at 0.5 % (a) , 2.5 % (c) , 4.5 % (e) , and 6 %.

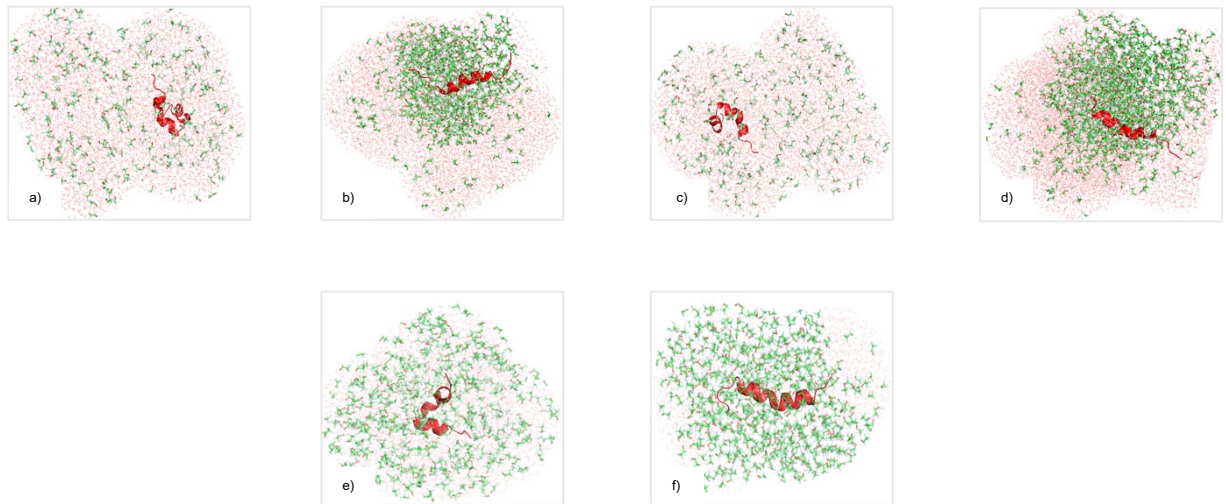


Figure S8. Representative snapshot of simulation within 0.6 nm from the melittin (RMLT) backbone in TFE-water system. Random coil structure of melittin at 10 % (a), 20 % (c), and 30 % (e) TFE-water system at the beginning of simulation. a -helix of melittin after 50 ns simulation in 10 % (b), 20 % (d) and 30 % (f) TFE-water system.

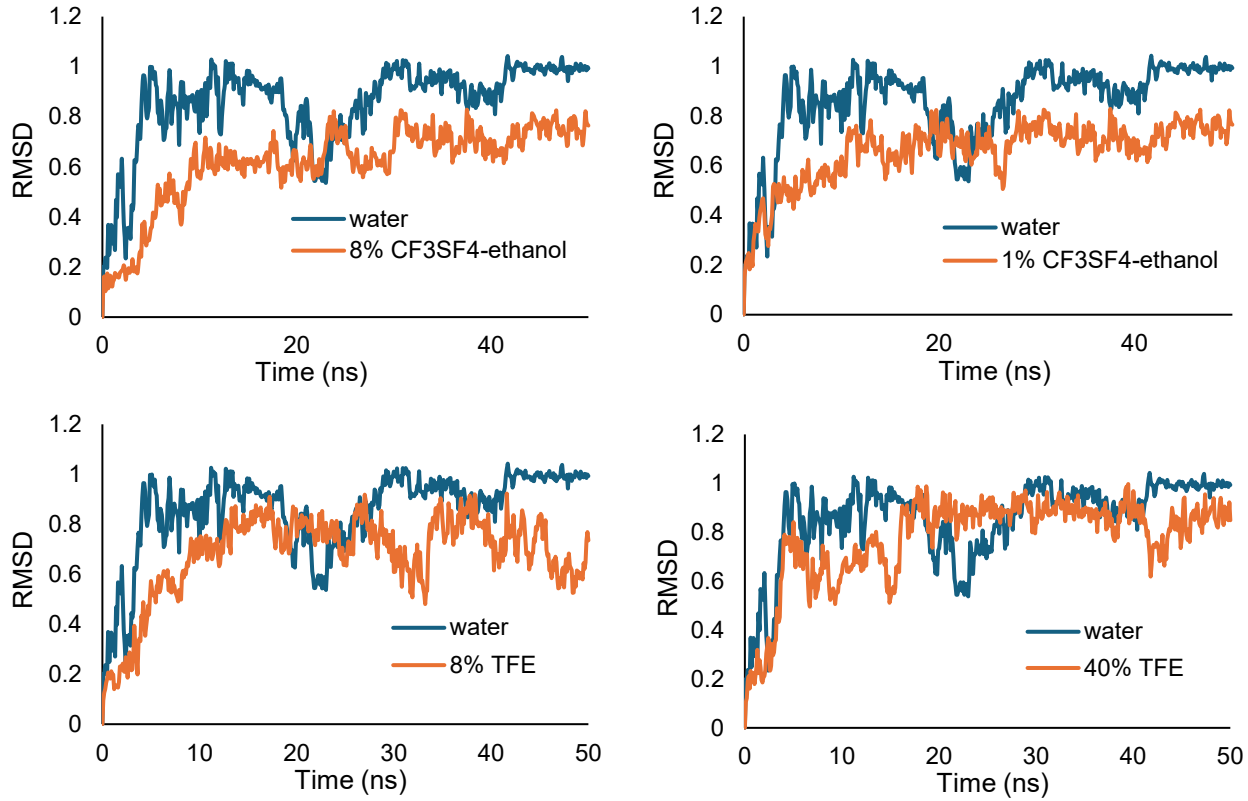


Figure S9. Backbone RMSD with respect to the initial simulated structure RMLT in 1%, 8% CF₃SF₄-ethanol-water and 8% and 40% TFE-water system for 50 ns simulation time.

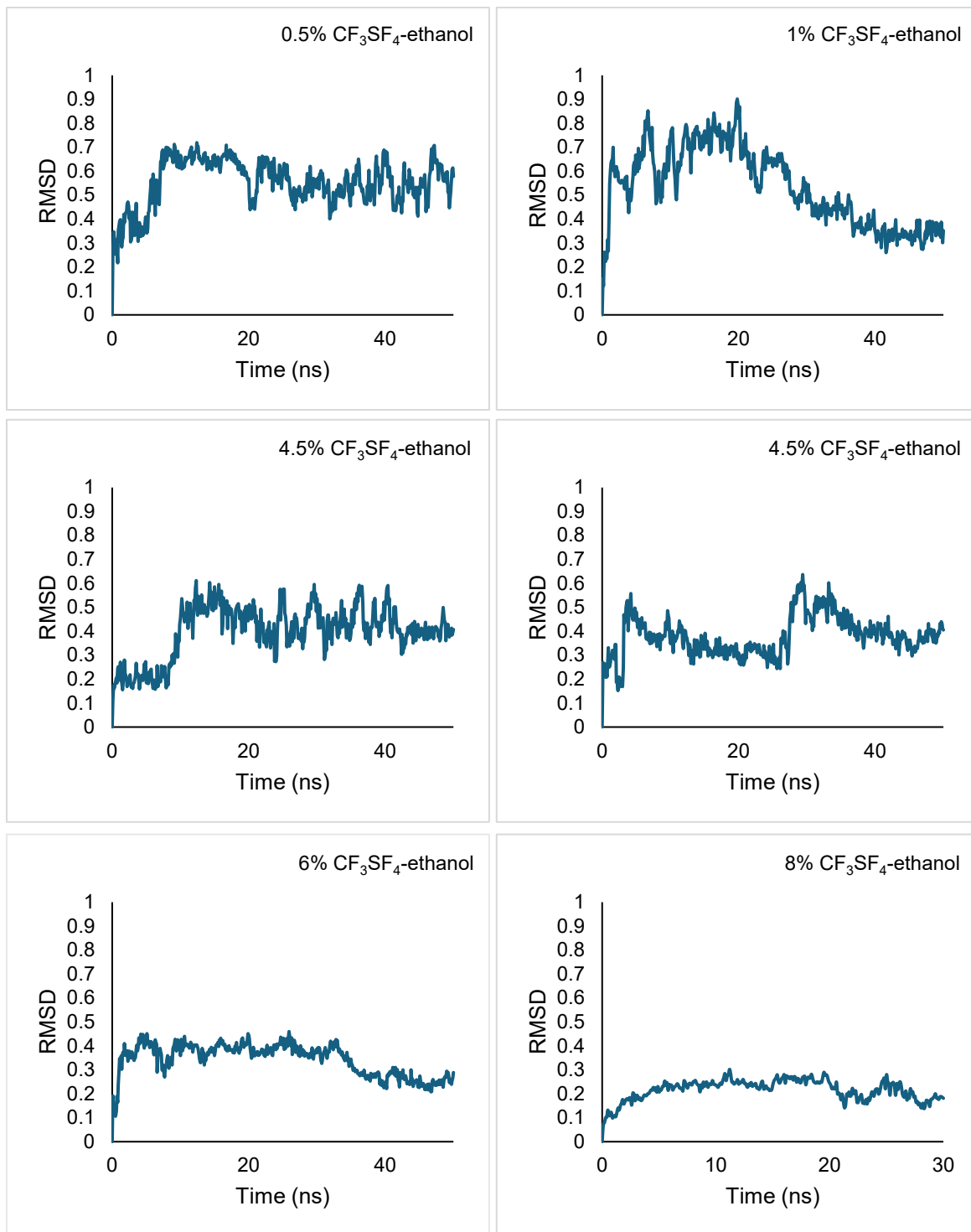


Figure S10. Backbone RMSD with respect to the initial structure of simulation of melittin (MLT) in CF_3SF_4 -ethanol for different concentrations.

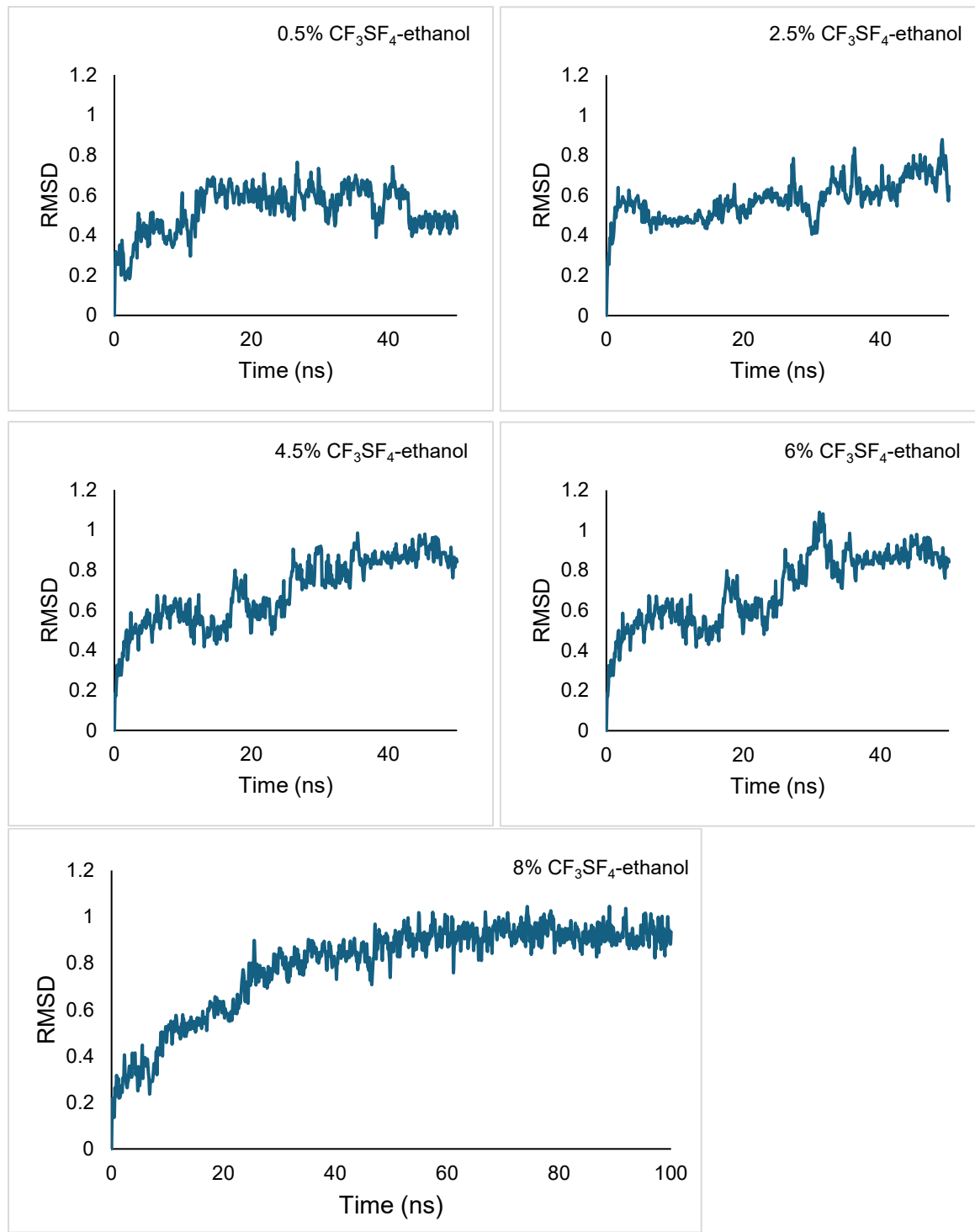


Figure S11. Backbone RMSD with respect to the initial structure of simulation of melittin (RMLT) in CF_3SF_4 -ethanol for different concentrations.

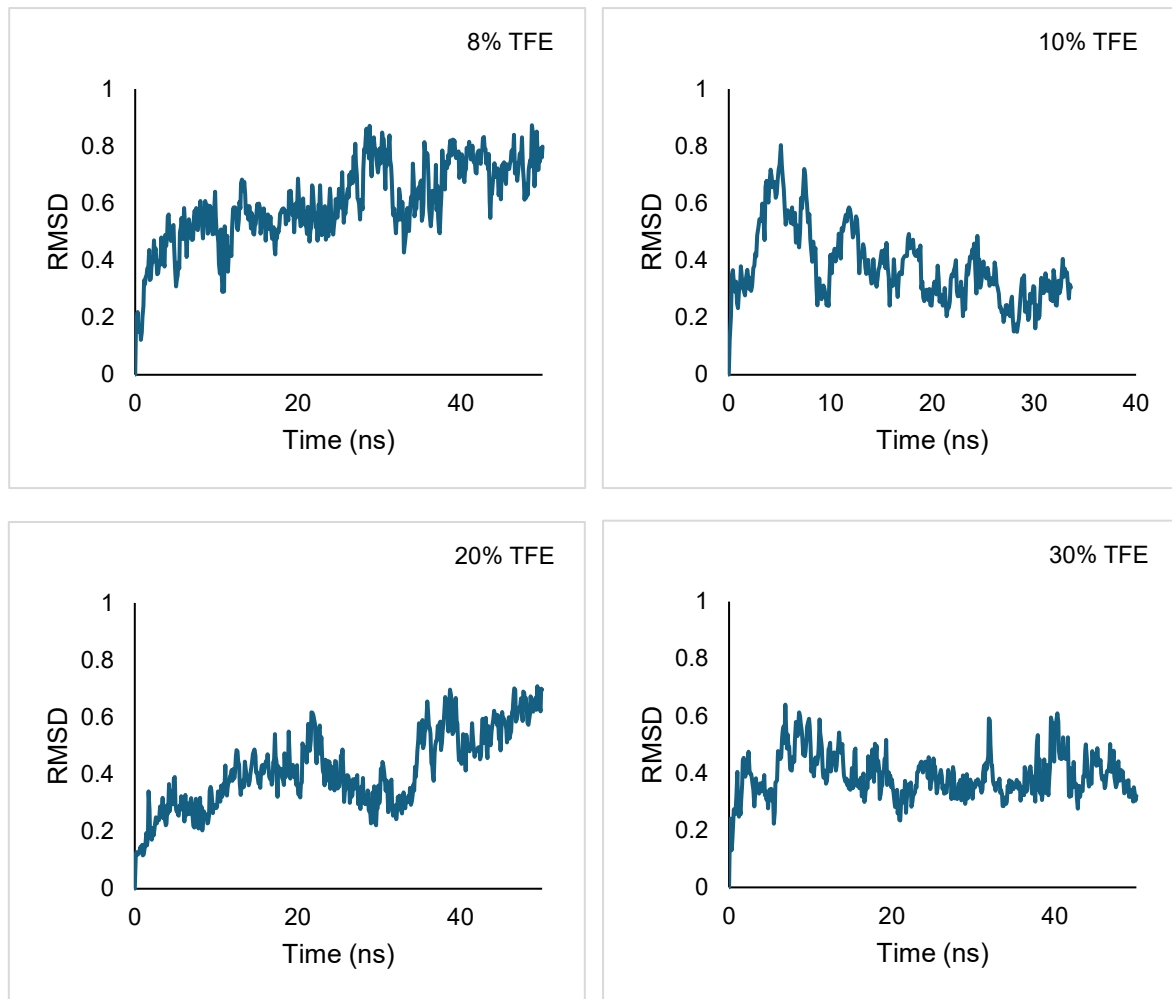


Figure S12. Backbone RMSD with respect to the initial structure of simulation of melittin (MLT) in TFE for different concentrations.

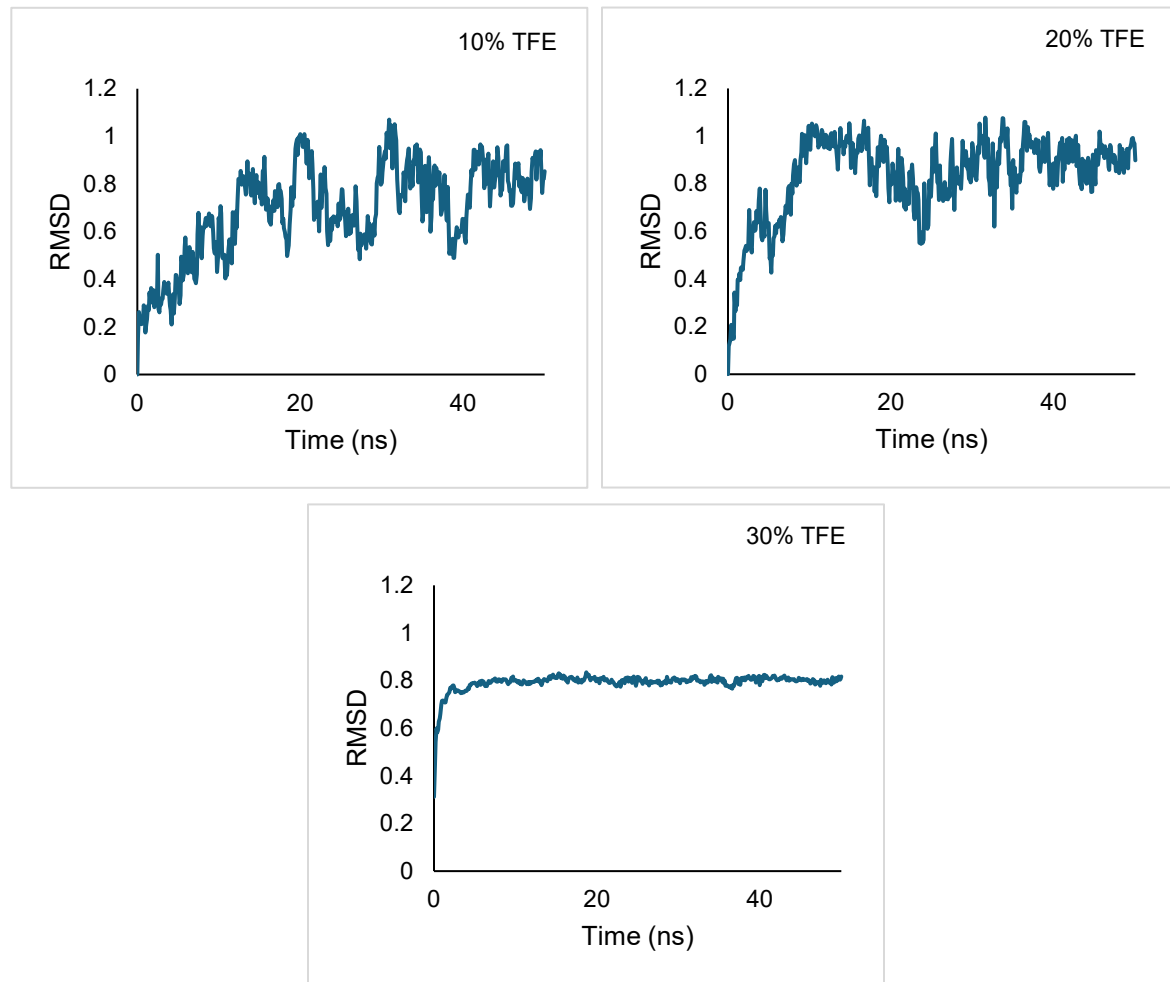


Figure S13. Backbone RMSD with respect to the initial structure of simulation of melittin (RMLT) in TFE for different concentrations.

<https://youtu.be/-fC3mkvGhSI>

Figure S14. Folding of RMLT in 8% CF₃SF₄-ethanol from 50 ns simulation.

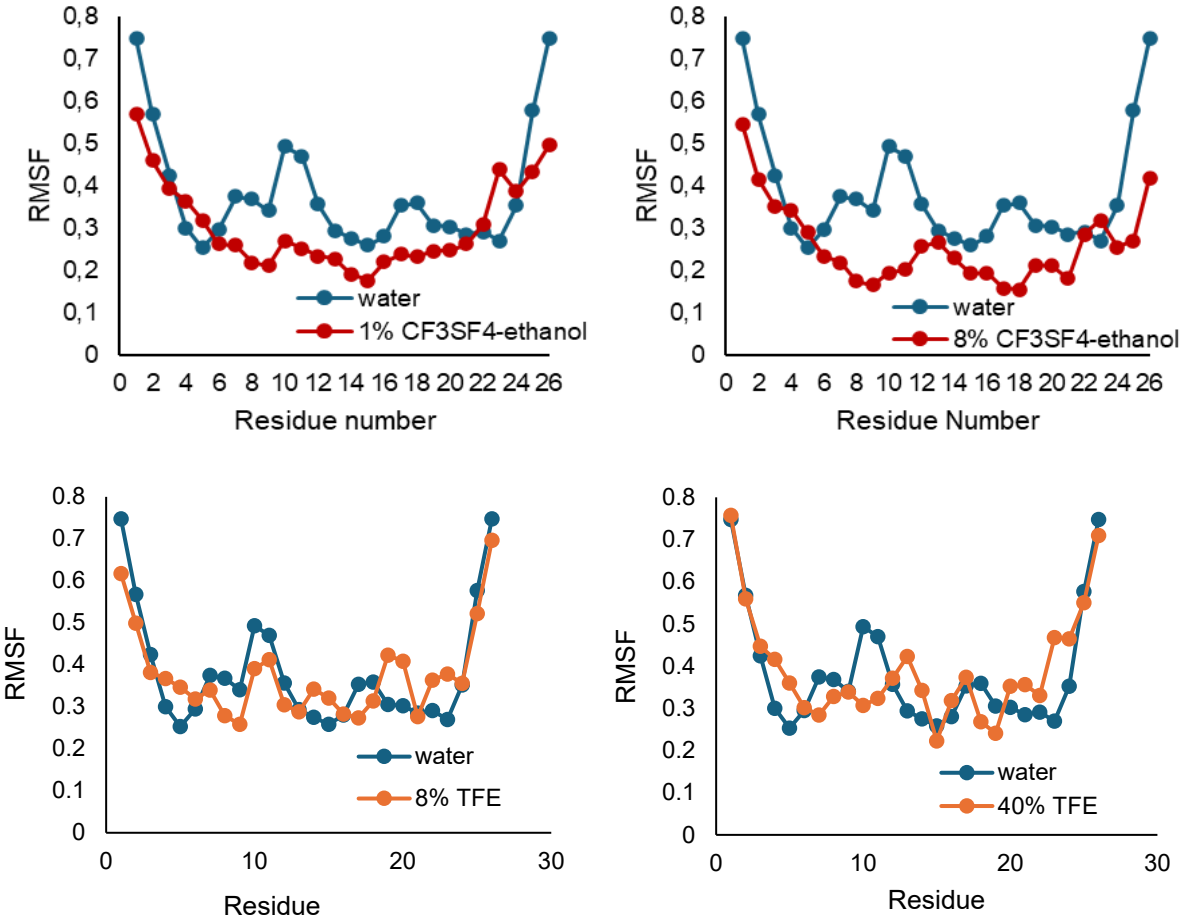


Figure S15. Backbone RMSF with respect to the structure RMLT in 1%, 8% CF₃SF₄-ethanol-water and 8% and 40% TFE-water system with respect to residue number.

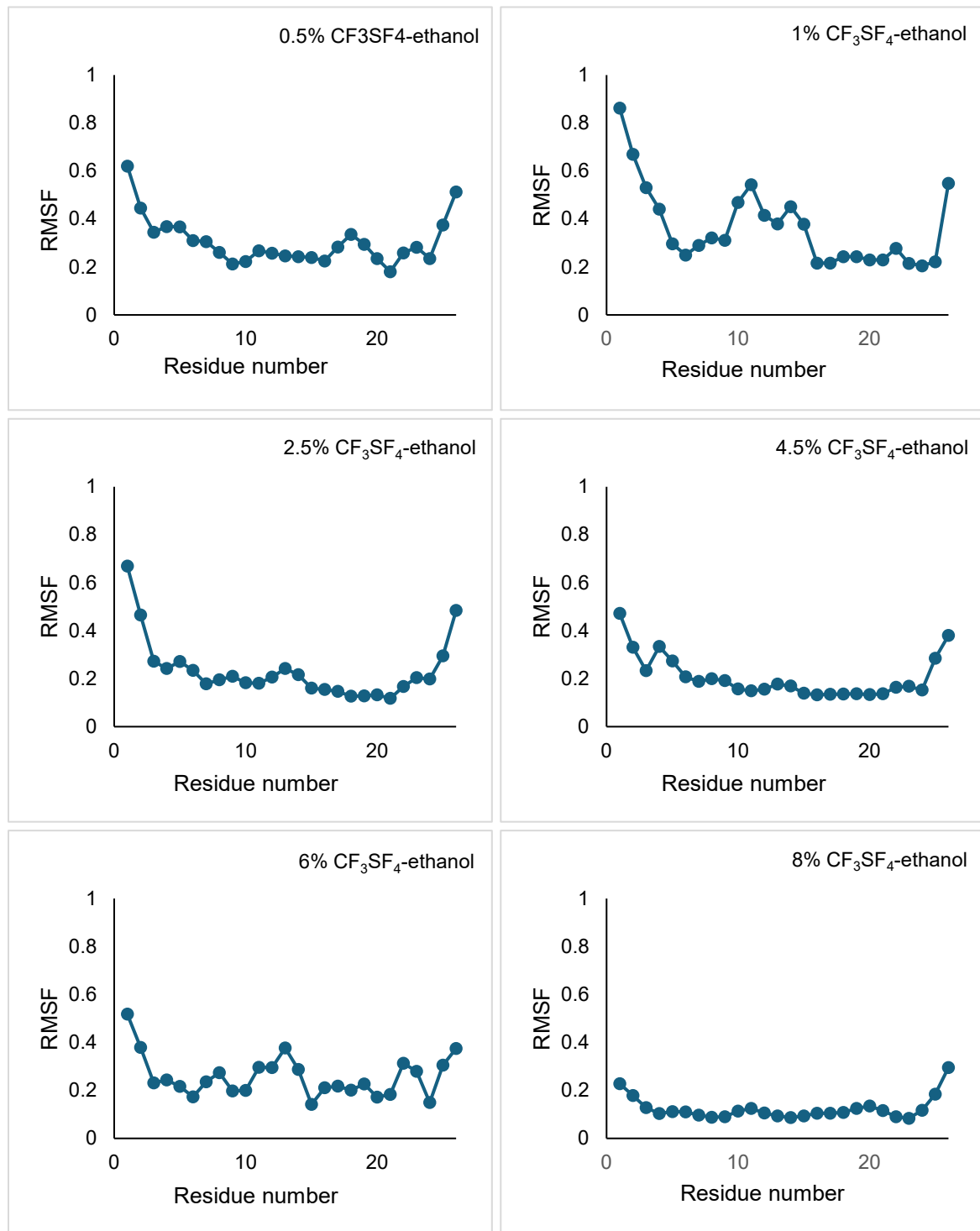


Figure S16. Backbone RMSF with respect to the initial structure of simulation of melittin (MLT) in CF_3SF_4 -ethanol for different concentrations.

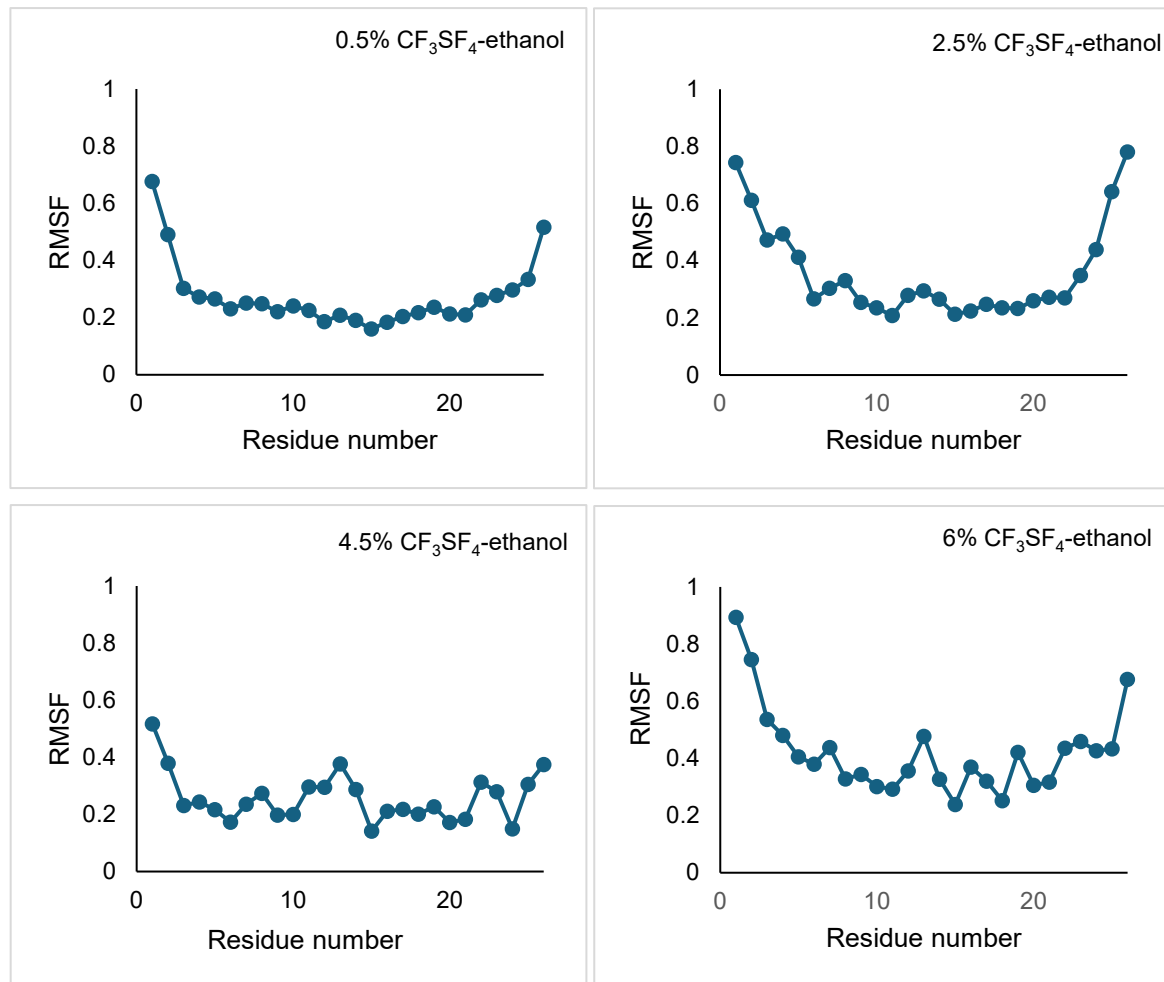


Figure S17. Backbone RMSF with respect to the initial structure of simulation of melittin (RMLT) in CF_3SF_4 -ethanol for different concentrations.

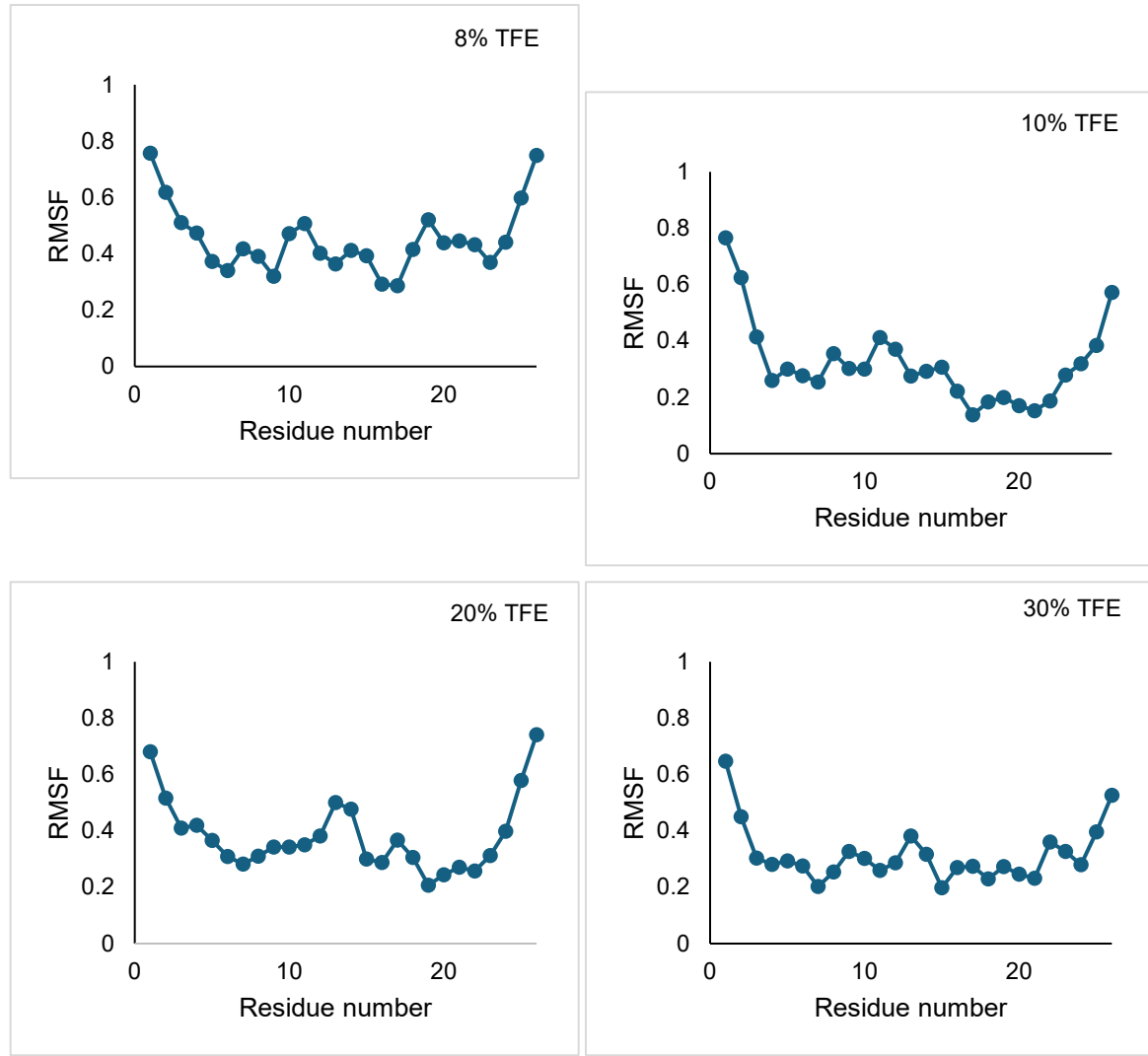


Figure S18. Backbone RMSF with respect to the initial structure of simulation of melittin (MLT) in TFE for different concentrations.

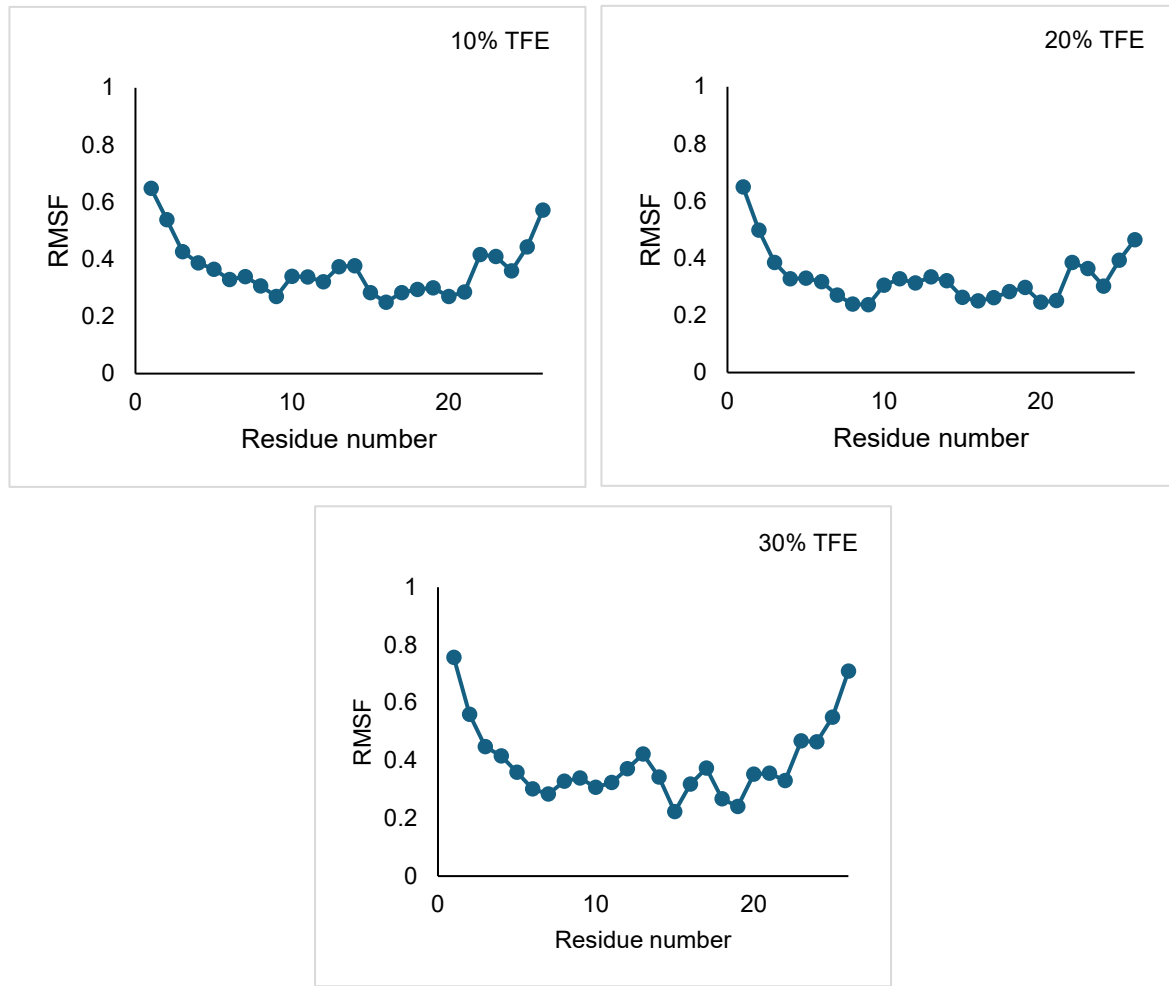


Figure S19. Backbone RMSF with respect to the initial structure of simulation of melittin (RMLT) in TFE for different concentrations.

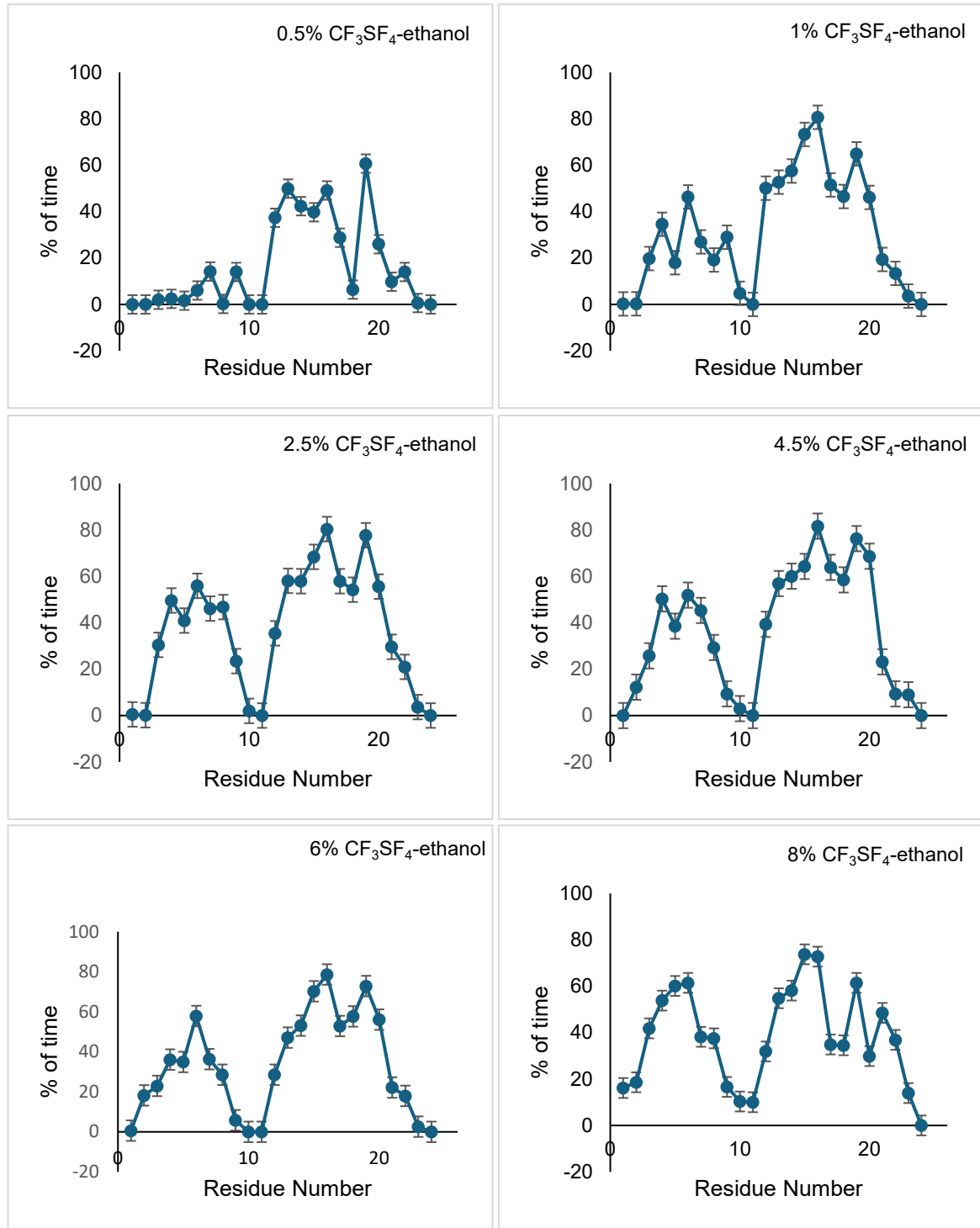


Figure S20. Helicity per residue with respect to % of time of melittin (MLT) in CF_3SF_4 -ethanol for different concentrations.

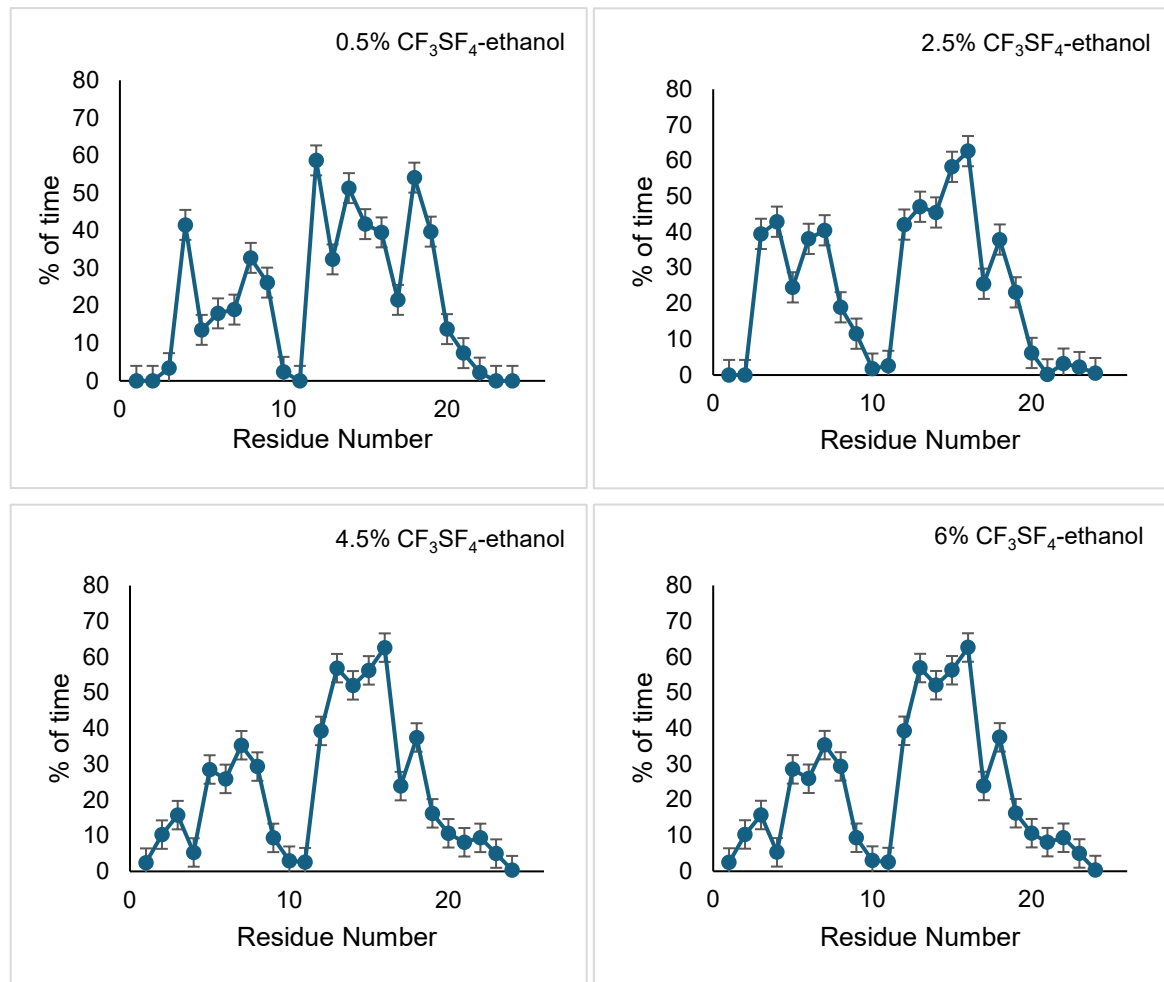


Figure S21. Helicity per residue with respect to % of time of melittin (RMLT) in $\text{CF}_3\text{SF}_4\text{-ethanol}$ for different concentrations.

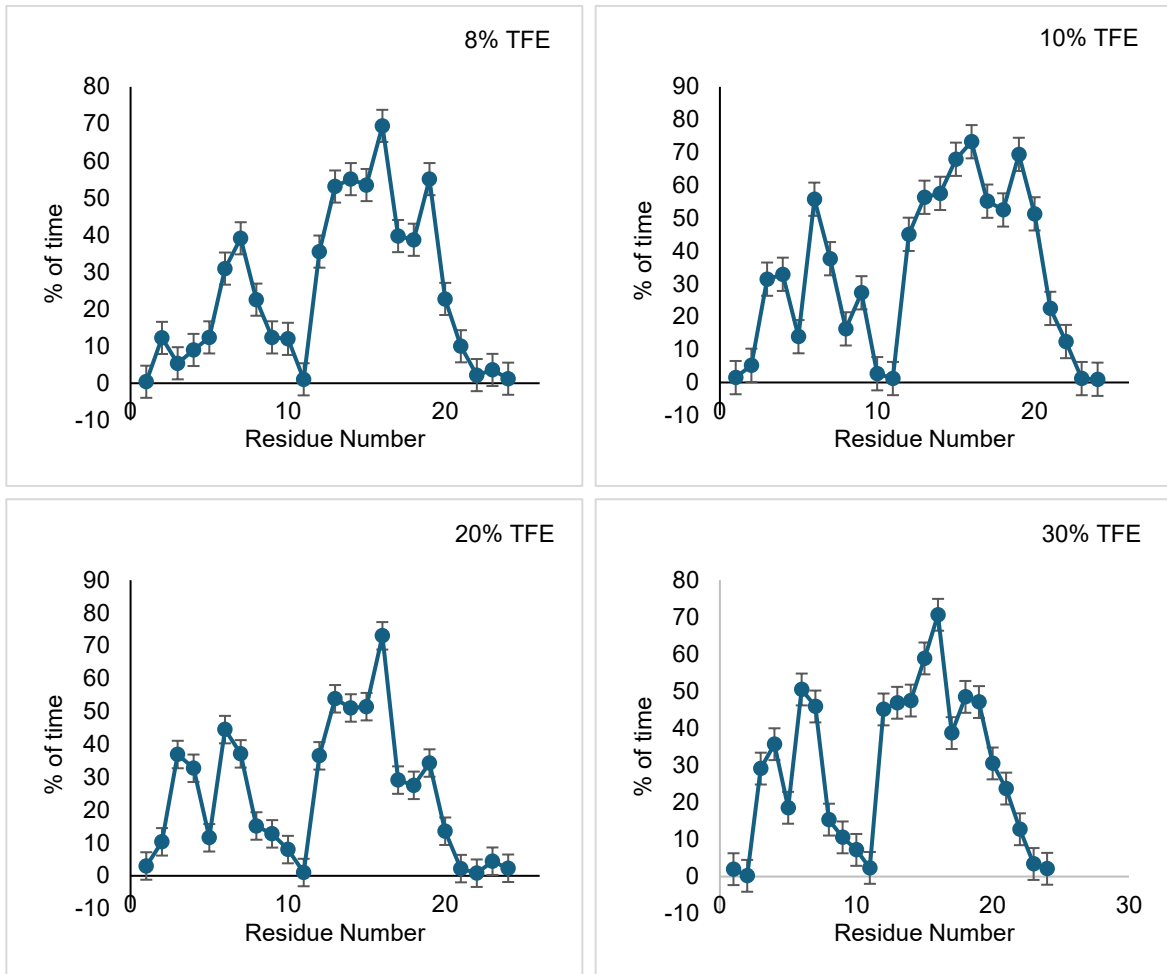


Figure S22. Helicity per residue with respect to % of time of melittin (MLT) in TFE for different concentrations.

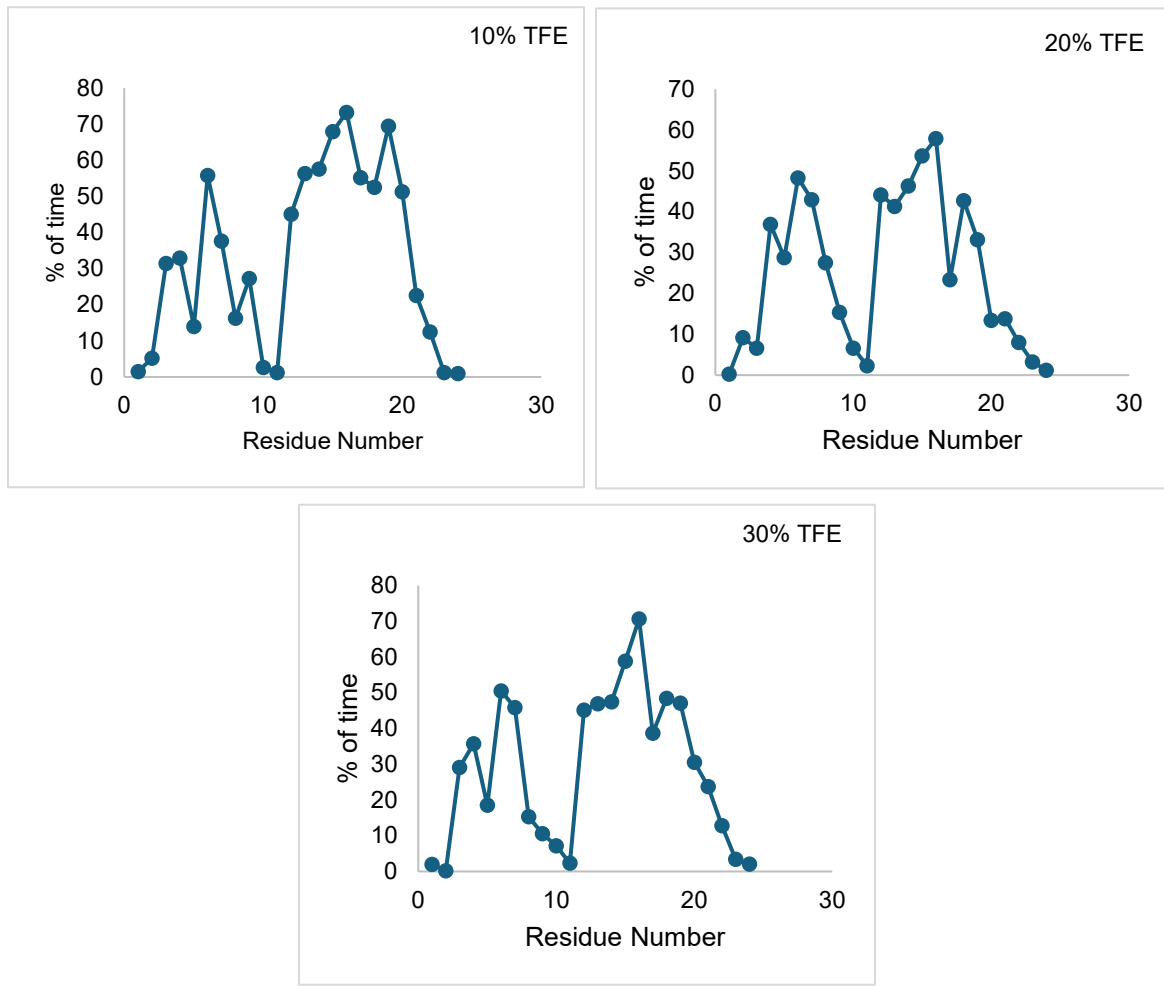


Figure S23. Helicity per residue with respect to % of time of melittin (RMLT) in TFE for different concentrations.

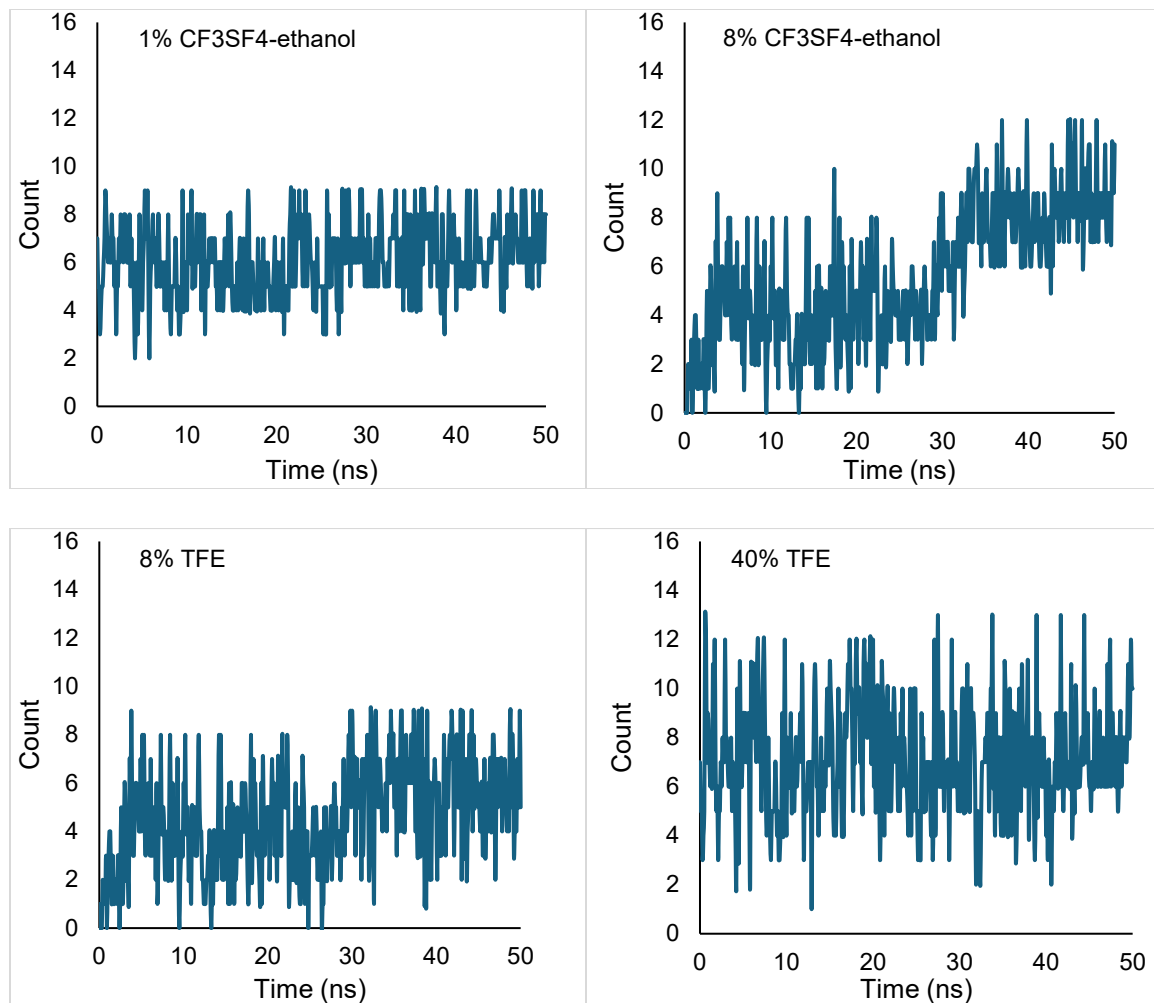


Figure. S24. Intermolecular hydrogen bonding interactions between the alcohols and the peptide over the period of the simulations.